

## Glutamate residue 90 in the predicted transmembrane domain 2 is crucial for cation flux through channelrhodopsin 2

Karelia Ruffert, Bettina Himmel, Deepti Lall, Christian Bamann, Ernst Bamberg, Heinrich Betz, Volker Eulenburg

### Angaben zur Veröffentlichung / Publication details:

Ruffert, Karelia, Bettina Himmel, Deepti Lall, Christian Bamann, Ernst Bamberg, Heinrich Betz, and Volker Eulenburg. 2011. "Glutamate residue 90 in the predicted transmembrane domain 2 is crucial for cation flux through channelrhodopsin 2." *Biochemical and Biophysical Research Communications* 410 (4): 737–43.  
<https://doi.org/10.1016/j.bbrc.2011.06.024>.

# Glutamate residue 90 in the predicted transmembrane domain 2 is crucial for cation flux through channelrhodopsin 2

Karelia Ruffert <sup>a,1</sup>, Bettina Himmel <sup>a,b,2</sup>, Deepti Lall <sup>a,3</sup>, Christian Bamann <sup>b</sup>, Ernst Bamberg <sup>b</sup>, Heinrich Betz <sup>a,\*</sup>, Volker Eulenburg <sup>a,\*</sup>

<sup>a</sup> Department of Neurochemistry, Max-Planck Institute for Brain Research, 60528 Frankfurt, Germany

<sup>b</sup> Department of Biophysical Chemistry, Max-Planck Institute of Biophysics, 60438 Frankfurt, Germany

## 1. Introduction

Channelrhodopsin 2 (ChR2) is a retinylidene protein of 737 amino acids that is expressed in the eye spot of the green alga *Chlamydomonas reinhardtii* and supposed to evoke photoresponses [1,2]. Illumination of *Xenopus laevis* oocytes expressing ChR2 with blue light ( $\lambda_{\text{max}} = 480$  nm) induces a transient peak current followed by a persisting stationary one, carried mainly by protons and other monovalent cations. Additionally,  $\text{Ca}^{2+}$ , but not  $\text{Mg}^{2+}$ , also permeates ChR2 [1,3]. The presumptive ion pore of ChR2 is located within the first 315 amino acids, as a correspondingly truncated ChR2 retains the electrophysiological properties of the full-length protein [1]. ChR2 shows 15–20% sequence homology to the microbial-type rhodopsins bacteriorhodopsin (BR), halorhodopsin (HR) and sensory rhodopsins (SRs). Their seven transmembrane domain structure [4–8] is consistent with hydropathy plots

of ChR2 [2], and spectroscopic data as well as measurements on lipid bilayers suggest that ChR2 is a leaky proton pump [9]. The precise topology, the mechanism of its proton pump activity, as well as the location of its ion channel pore, however, remain elusive.

Here, we investigated whether a cluster of glutamates localized at positions 90, 97 and 101 of the predicted TM2 of ChR2 is implicated in ion permeation and/or cation selectivity. Neutral substitution of E97 has been previously shown to result in modest changes in current amplitude [10]. We report that charge inversions at these positions impair ChR2 currents, and that residue E90 appears to be particularly important for both  $\text{H}^+$  and  $\text{Na}^+$  conductance. Our results suggest that TM2 contributes to the lining and selectivity filter of ChR2's intrinsic ion channel.

## 2. Materials and methods

### 2.1. Plasmids and cRNA synthesis

cDNAs encoding a truncated version of ChR2 (AA1–315) or a C-terminal fusion of the truncated ChR2 sequence to YFP (ChR2-YFP; see [1]) were cloned into pGemHE [11] using its BamHI and XhoI sites. Mutations were introduced by site-directed mutagenesis using the QuickChange Mutagenesis Kit (Agilent Technologies, Santa Clara, USA) and confirmed by sequencing. After linearization at a unique NheI site, these ChR2-encoding plasmids were used as templates for cRNA synthesis with the mMessage T7 Ultra Kit (Ambion, Austin, USA).

\* Corresponding authors. Present address: Max-Planck Institute for Medical Research, Jahnstrasse 29, 69120 Heidelberg, Germany (H. Betz). Institute for Biochemistry and Molecular Medicine, University Erlangen-Nürnberg, Fahrstrasse 17, 91054 Erlangen, Germany (V. Eulenburg).

E-mail addresses: [Heinrich.Betz@mpimf-heidelberg.mpg.de](mailto:Heinrich.Betz@mpimf-heidelberg.mpg.de) (H. Betz), [Volker.Eulenburg@biochem.uni-erlangen.de](mailto:Volker.Eulenburg@biochem.uni-erlangen.de) (V. Eulenburg).

<sup>1</sup> Present address: Faculté des Sciences Pharmaceutiques et Biologiques, University Paris Descartes, 75006 Paris, France.

<sup>2</sup> Present address: Merz Pharmaceuticals GmbH, 60318 Frankfurt, Germany.

<sup>3</sup> Present address: Institute for Biochemistry and Molecular Medicine, University Erlangen-Nürnberg, 91054 Erlangen, Germany.

## 2.2. Oocyte preparation and cRNA injection

*Xenopus laevis* oocytes were isolated and maintained as described [12,13]. Oocytes were injected with approximately 20 ng of cRNA and incubated at 18 °C for 3 days in standard ND96 (in mM: NaCl 96, KCl 2, MgCl<sub>2</sub> 1, CaCl<sub>2</sub> 1, Hepes/NaOH 5; pH 7.4; 50 µg/ml gentamycin) containing 1 µM *all-trans*-retinal. Non-injected oocytes from the same batch incubated in parallel were used as controls.

## 2.3. Electrophysiology

Two-electrode voltage-clamp (TEVC) recordings from oocytes were performed using a Turbo TEC-03X amplifier and CellWorks (V3.7) data acquisition software (all from npi, Göttingen, Germany) as described previously [14]. Chr2 currents were induced by illumination with an HBO 100 lamp (Zeiss, Göttingen, Germany) equipped with a band pass filter (450 ± 25 nm, AHF Analysentechnik, Göttingen, Germany). Light was focussed by a lens on a 2 mm light guiding fiber (PG-R-FB1500; Laser Components, Olching, Germany). Illumination was controlled by a computer-triggered shutter (Uniblitz VCM-D1; Vincent Associates, Rochester, USA).

Routinely, oocytes were held at a membrane potential ( $V_m$ ) of -60 mV. Transmembrane voltage changes from -80 to +40 mV were applied in 20 mV steps. After holding the respective  $V_m$  for 1.5 s, illumination was for 3 s; 1.5 s after termination of the light pulse, the membrane potential was changed to a new  $V_m$ . Oocytes were superfused successively with Na<sup>+</sup> or *N*-methyl-glucamine (NMG) containing buffers (in mM: NaCl 110 or NMG 110; MgCl<sub>2</sub> 2; Hepes 5, adjusted to pH 4.0 (Na4.0), 7.6 (Na7.6) or 9.0 (Na9.0) with HCl or NaOH, respectively).

## 2.4. Data evaluation

Current values were determined using CellWorks (V3.7) software. Mean values (±SEM) were calculated from 8 to 18 TEVC-measurements obtained with oocytes from at least three frogs. For *I/V*-relation curves, absolute values were normalized to Na7.6, if not indicated otherwise.

## 3. Results

### 3.1. Charged residues in TM2 might form an amphipathic helix

To identify residues of Chr2 that could be involved in the formation of the ion channel, we aligned Chr2 to Chr1, another light-gated channel protein from *Chlamydomonas reinhardtii* originally thought to be H<sup>+</sup>-selective [15,16]. Assuming that membrane permeating cations should be stabilized by hydrophilic or negatively charged side chains, we identified three glutamate residues, E90, E97 and E101, within the predicted  $\alpha$ -helical TM2 (Fig. 1A; see also Refs. [2,10]). These residues and a lysine residue at position 93 are conserved in both Chr2 and Chr1 but absent in BR, which acts exclusively as a proton pump [17]. The side chains of these charged residues are predicted to lie at one side of the TM2  $\alpha$ -helix and thus could create a negatively charged hydrophilic microdomain within the transmembrane core of Chr2 (Fig. 1B).

### 3.2. Characteristics of light-induced Chr2 currents

A truncated version of Chr2 lacking the large intracellular C-terminal domain (Chr2<sub>1-315</sub>) has been shown to generate photocurrents identical to that of the full-length protein [1], and a fluorescent fusion protein of Chr2<sub>1-315</sub> (Chr2-YFP) is widely used for light-induced manipulation of neuronal activity [18–20]. To

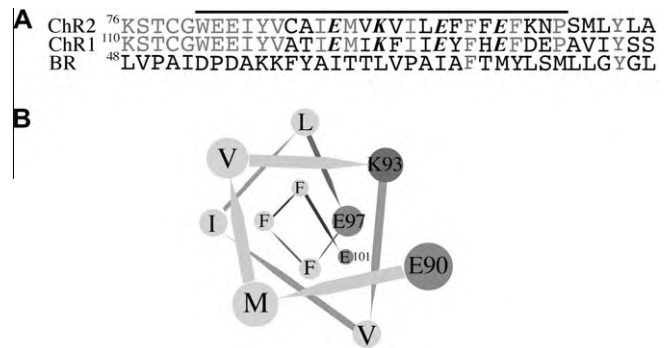


**Fig. 1.** Amphipathic nature of the putative TM2 region of Chr2. (A) Alignment of partial amino acid sequences including the putative TM2 regions (black bar) of Chr2, Chr1 and BR. Conserved amino acids are indicated in gray. Charged TM2 residues found in both Chr2 and Chr1, but not in BR, are shown in bold italics. (B)  $\alpha$ -Helical wheel plot of the TM2 residues 90–101 of Chr2 viewed from the intra- to the extracellular side. Note that all charged side chains (E90, K93, E97 and E101, highlighted in dark gray) face one side of the putative  $\alpha$ -helix.

facilitate the eventual usage of mutants with altered ion conductance for biological applications, we generated all substitutions in the Chr2-YFP construct. In all our recordings, the properties of Chr2-YFP were indistinguishable from those of the unfused Chr2<sub>1-315</sub> protein (compare Fig. 2A, B and Supplementary Fig. S1; see also Table 1).

Illumination of Chr2-YFP expressing oocytes held at a  $V_m$  of -80 mV in NaCl solution at pH 7.6 (Na7.6) induced a biphasic, inwardly directed current consisting of a transient and a stationary component that persisted until the end of the light pulse (Fig. 2A; see also Ref. [1]). Non-injected control oocytes did not display light-induced currents (data not shown). At +40 mV, current flow was outwardly directed (Fig. 2A). The current-voltage (*I/V*) analysis of these light-induced currents disclosed a pronounced inward rectification with a reversal potential ( $V_{rev}$ ) of  $-9 \pm 2$  mV (Fig. 2B and Table 1).

To determine the contribution of different cations to the total Chr2-mediated current, we used buffers containing different H<sup>+</sup> and Na<sup>+</sup> concentrations. When decreasing the external H<sup>+</sup> concentration to pH 9.0 (Na9.0), only a small reduction of the inward currents was observed at negative membrane potentials, and the  $V_{rev}$  values were not significantly altered (Fig. 2B). This is consistent with Chr2-mediated inward currents at neutral and alkaline pH being predominantly carried by Na<sup>+</sup> ions. In contrast, at pH 4.0 light-induced currents were increased and only inwardly-directed at all membrane potentials analyzed (Fig. 2B). Apparently H<sup>+</sup> is the predominantly conducted ion species in Na4.0. This interpretation was confirmed by analyzing the *I/V*-relations derived from Chr2-YFP expressing oocytes superfused with solutions, in which Na<sup>+</sup> was replaced by NMG. The currents generated in NMG4.0 were not significantly different from those obtained upon Na4.0 superfusion (Fig. 2B and Table 1). However, when the external H<sup>+</sup>-concentration was decreased to pH 9.0 in the absence of Na<sup>+</sup> (NMG9.0), only small light-induced currents were detected, and  $V_{rev}$  was shifted to strongly negative membrane potentials (Table 1). The outwardly directed currents in NMG7.6 and NMG9.0 most likely resulted from Chr2-mediated cation efflux, probably K<sup>+</sup>, as observed in recordings from Na7.6 or Na9.0 superfused oocytes held at positive  $V_m$  (Fig. 2B). Since the absorption spectrum of Chr2 is insensitive to changes in pH [21], the different current amplitudes cannot be attributed to changes in excitation wavelength sensitivity.

### 3.3. Charge inversion of TM2 glutamates impairs Chr2 currents

To investigate whether the residues E90, E97 and E101 contribute to Chr2 conductance and/or ion selectivity, we generated the

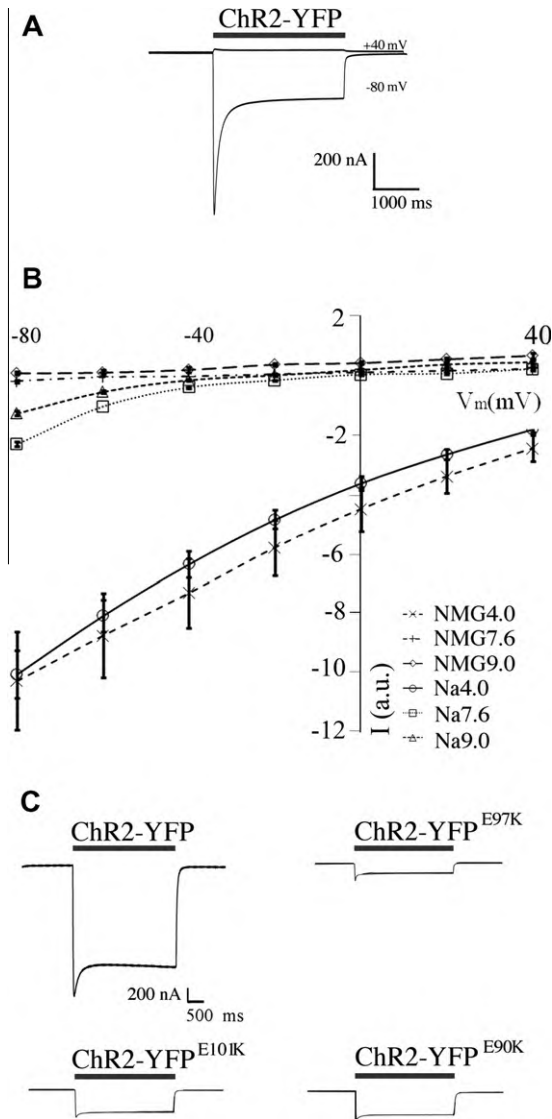


**Fig. 2.** Light-induced currents of ChR2-YFP and ChR2-YFP charge inversion mutants. (A) TEVC recording from an oocyte expressing ChR2-YFP in Na7.6. Photocurrents were registered at  $V_m$  of  $-80$  and  $+40$  mV. The gray bar indicates illumination with blue light. (B) Normalized  $I/V$ -relationships of stationary photocurrents recorded from ChR2-YFP expressing oocytes in Na4.0, Na7.6, Na9.0, NMG4.0, NMG7.6 and NMG9.0. Current values were normalized to the amplitudes recorded in Na7.6 at  $-60$  mV (a.u. = arbitrary units). (C) TEVC traces recorded from oocytes expressing ChR2-YFP, ChR2-YFP<sup>E101K</sup>, ChR2-YFP<sup>E97K</sup> and ChR2-YFP<sup>E90K</sup> at  $V_m = -80$  mV in Na4.0. Illumination is indicated by gray bars.

charge inversion mutants ChR2-YFP<sup>E90K</sup>, ChR2-YFP<sup>E97K</sup> and ChR2-YFP<sup>E101K</sup> (Fig. 2C). Oocytes expressing ChR2-YFP<sup>E90K</sup>, ChR2-YFP<sup>E97K</sup> and ChR2-YFP<sup>E101K</sup> did not produce detectable photocurrents in buffers at pH 7.6 or pH 9.0, indicating that these substitutions severely impaired channel function (data not shown). However, in Na4.0 and NMG4.0 light-induced currents were observed, although the amplitudes of the stationary currents were strongly reduced as compared to the wild-type ChR2-YFP protein (Fig. 2C and Table 1). Notably, substitution of the conserved lysine residue K93 by glutamate or alanine also impaired light-induced currents (data not shown); this is consistent with residues E90, K93, E97 and E101 forming a crucial amphipathic  $\alpha$ -helix.

$I/V$ -relations of ChR2-YFP<sup>E97K</sup> and ChR2-YFP<sup>E101K</sup> mediated currents indicated reversal potentials of  $>+40$  mV, i.e. similar to those of the wild-type ChR2-YFP protein. However, the  $V_{rev}$  of ChR2-YFP<sup>E90K</sup> was shifted to more negative values, i.e. close to 0 mV

(Table 1; see also Fig. 3). This shift in  $V_{rev}$  suggested qualitative changes in the channel properties upon substitution of E90. Therefore, we concentrated on this residue for a more detailed analysis.

### 3.4. E90 is important for the cation conductance of ChR2

Unlike the charge inversion in ChR2-YFP<sup>E90K</sup>, replacement of E90 by the polar amino acid glutamine (ChR2-YFP<sup>E90Q</sup>) resulted in only moderate changes, namely a small reduction of light-induced transient and stationary currents in all buffers analyzed (Fig. 3 and Table 1). The stationary currents determined in Na7.6 and Na9.0 were reduced to  $46 \pm 7\%$  and  $59 \pm 14\%$ , respectively, as compared to the wild-type ChR2-YFP current (Fig. 3A and Table 1). More pronounced reductions in light-induced current amplitudes were observed upon superfusion with NMG4.0 or Na4.0 ( $25 \pm 5\%$  and  $26 \pm 5\%$ , respectively, as compared to ChR2-YFP; Fig. 3A, B and Table 1). Qualitatively, however, the  $I/V$ -relations of the normalized stationary currents recorded from ChR2-YFP<sup>E90Q</sup>-expressing oocytes were only slightly altered (compare Figs. 2B and 3B); this is consistent with spectroscopic data showing that the photocycle of this mutant is not significantly disturbed [22].

To unravel whether a polar side chain at position 90 is necessary for proper ChR2 function, we replaced E90 by alanine. Oocytes expressing ChR2-YFP<sup>E90A</sup> produced larger light-induced currents than ChR2-YFP expressing oocytes in Na7.6 (data not shown, but see Table 1) or in Na9.0 (Fig. 3C and Table 1), indicating that this mutant is fully functional.  $I/V$  relations determined in these buffers were nearly indistinguishable between mutant and wild-type (compare Figs. 2B and 3D). This is consistent with these currents being predominantly mediated by Na<sup>+</sup>. Notably, in NMG4.0 ChR2-YFP<sup>E90A</sup> mediated currents were strongly reduced as compared to those carried by ChR2-YFP and even smaller than the currents registered from the same oocyte upon Na9.0 superfusion (Fig. 3C). Thus, the E90A substitution reduces the H<sup>+</sup> conductance of ChR2-YFP. In buffers containing high H<sup>+</sup> concentrations and Na<sup>+</sup> (Na4.0), light-induced currents mediated by ChR2-YFP<sup>E90A</sup> were almost identical to those seen in NMG4.0. Apparently, high H<sup>+</sup> concentrations inhibit the Na<sup>+</sup>-conductance of ChR2-YFP<sup>E90A</sup>. Notably, its  $V_{rev}$  values determined in NMG4.0 and Na4.0 were rather similar ( $+11 \pm 5$  mV and  $+14 \pm 1$  mV, respectively; Table 1 and Fig. 3D). Apparently currents were carried by the same ion species in both buffers.

To exclude that changes in the ChR2 photocycle are responsible for the reduced currents observed at pH 4.0, we also analyzed the photocycle kinetics spectroscopically (Supplementary Fig. S2). No significant differences were observed between ChR2-YFP<sup>E90A</sup> and ChR2-YFP, suggesting that E90 is not involved in the photoreaction.

Comparison of the light-induced currents recorded from ChR2-YFP<sup>E90A</sup> and ChR2-YFP<sup>E90K</sup> expressing oocytes revealed that the  $I/V$  relations of both mutants were almost identical at pH 4.0 (see Na4.0 and NMG4.0 in Fig. 3E and F). Interestingly, and unlike ChR2-YFP<sup>E90A</sup>, we failed to observe any predominantly Na<sup>+</sup>-mediated currents of ChR2-YFP<sup>E90K</sup> in Na7.6 or Na9.0 (Fig. 3E). This indicates that substitution of E90 by lysine but not alanine renders ChR2 Na<sup>+</sup>-impermeable. Additionally, ChR2-YFP<sup>E90K</sup> displays a strongly reduced H<sup>+</sup>-conductance. The observed changes in  $V_{rev}$  ( $1 \pm 3$  mV in Na4.0, and  $-1 \pm 3$  mV in NMG4.0; Fig. 3F and Table 1) further suggest that additional ions might contribute to the small light-induced currents observed at pH 4.0. In summary, E90 is crucial for both the Na<sup>+</sup>- and H<sup>+</sup>-conductance of ChR2.

### 3.5. pH dependence of ChR2-YFP<sup>E90A</sup> mediated currents

As described above, the Na<sup>+</sup> conductance of ChR2-YFP<sup>E90A</sup> appeared to be inhibited by high external H<sup>+</sup> concentrations. Therefore, the pH dependence of the light-induced currents was

**Table 1**

Current amplitudes and  $V_{rev}$  values of ChR2-YFP mutants. Mean stationary currents recorded at a  $V_m$  of  $-80$  mV ( $I_{(-80mV\ stat)}$ ) and  $V_{rev}$  values calculated from oocytes expressing ChR2, ChR2-YFP, ChR2-YFP<sup>E90</sup>, ChR2-YFP<sup>E97</sup>, or ChR2-YFP<sup>E101</sup>, respectively, were determined in the buffers indicated ( $n \geq 8$ ). n.d., no detectable current.

Protein	Buffer	$I_{-80mV\ stat.}$ (nA)	% of ChR2-YFP	$V_{rev}$ (mV)
ChR2	NMG4	$-1902 \pm 637$		$>+40$
	Na4	$-1831 \pm 492$		$>+40$
	Na7.6	$-394 \pm 81$		$-23 \pm 6$
	NMG9	$+20 \pm 13$		$<-80$
	Na9	$-308 \pm 69$		$-25 \pm 3$
ChR2-YFP	NMG4	$-1878 \pm 595$		$>+40$
	Na4	$-1292 \pm 424$		$>+40$
	Na7.6	$-362 \pm 114$		$-9 \pm 2$
	NMG9	$+30 \pm 16$		$>-80$
	Na9	$-170 \pm 39$		$-27 \pm 5$
ChR2-YFP <sup>E90Q</sup>	NMG4	$-461 \pm 85$	$25 \pm 5$	$>+40$
	Na4	$-340 \pm 84$	$26 \pm 7$	$>+40$
	Na7.6	$-168 \pm 27$	$46 \pm 8$	$-6 \pm 3$
	NMG9	n.d.	n.d.	
	Na9	$-101 \pm 1$	$59 \pm 0.6$	$-42 \pm 12$
ChR2-YFP <sup>E90A</sup>	NMG4	$-138 \pm 21$	$7 \pm 0.4$	$+11 \pm 12$
	Na4	$-143 \pm 23$	$11 \pm 2$	$+14 \pm 1$
	Na7.6	$-635 \pm 95$	$176 \pm 26$	$-8 \pm 1$
	NMG9	$+4 \pm 6$	$12 \pm 20$	$<-80$
	Na9	$-582 \pm 73$	$343 \pm 43$	$+3 \pm 10$
ChR2-YFP <sup>E90K</sup>	NMG4	$-343 \pm 150$	$18 \pm 8$	$+4 \pm 2$
	Na4	$-187 \pm 67$	$19 \pm 5$	$-1 \pm 3$
	Na7.6	n.d.	n.d.	n.d.
	NMG9	n.d.	n.d.	n.d.
	Na9	n.d.	n.d.	n.d.
ChR2-YFP <sup>E97K</sup>	NMG4	$-108 \pm 40$	$6 \pm 2$	$>+40$
	Na4	$-55 \pm 7$	$4 \pm 0.5$	$>+40$
	Na7.6	n.d.	n.d.	n.d.
	NMG9	n.d.	n.d.	n.d.
	Na9	n.d.	n.d.	n.d.
ChR2-YFP <sup>E101K</sup>	NMG4	$-337 \pm 55$	$18 \pm 3$	$>+40$
	Na4	$-207 \pm 32$	$16 \pm 3$	$>+40$
	Na7.6	n.d.	n.d.	n.d.
	NMG9	n.d.	n.d.	n.d.
	Na9	n.d.	n.d.	n.d.

investigated in more detail for both ChR2-YFP<sup>E90A</sup> and ChR2-YFP by recording at pH values of 7.6, 6.4, 5.2 and 4.0 in both NaCl and NMG containing buffers. Consistent with our previous observations, acidification resulted in an increase in the slope of the  $I/V$  curves and rightward shifts of the  $V_{rev}$  values of ChR2-YFP in both NaCl and NMG containing buffers (Fig. 4A and data not shown). In contrast, with ChR2-YFP<sup>E90A</sup> expressing oocytes  $V_{rev}$  values were only slightly shifted to more positive values when the extracellular pH was lowered (Fig. 4B;  $V_{rev}$  at pH 4.0 close to 0 mV as compared to  $>+40$  mV for ChR2-YFP).

To determine the contribution of Na<sup>+</sup> ions to total current, we evaluated the changes of the sodium component of light-induced currents, as determined by the difference in current amplitudes in the presence and absence of Na<sup>+</sup> ions, at different pH values (Fig. 4C and D). For ChR2-YFP, we observed only moderate differences between pH 7.6 and 5.2. At pH 4.0, however, an outwardly directed Na<sup>+</sup> component of the light-induced current, most likely reflecting inhibition of H<sup>+</sup> mediated currents by Na<sup>+</sup>, appeared which resembled that described for voltage-gated sodium channels [23]. In contrast, with ChR2-YFP<sup>E90A</sup> the Na<sup>+</sup> component of the light-induced currents was barely detectable upon acidification of the superfusion solution (Fig. 4D), in line with the reduction in total current (Fig. 4B). This indicates that ChR2-YFP<sup>E90A</sup> is poorly permeable for Na<sup>+</sup> at low pH.

#### 4. Discussion

In this study, we investigated whether three glutamate residues located within the predicted TM2 of ChR2 contribute to the chan-

nel-like cation conductance of this light-activated proton pump. Based on hydropathy plots and sequence comparison with ChR1 and BR, we identified four charged amino acids (E90, K93, E97 and E101) within the putative TM2 that might form an amphipathic helix suitable to provide for hydrophilic lining of the leak channel of ChR2. Assuming an  $\alpha$ -helical arrangement of TM2, these residues are likely to be oriented away from the hydrophobic environment of the lipid bilayer and to lie within the center of the putative 7-TM helical bundle of ChR2.

The charged residues within TM2 are conserved between ChR1 and ChR2, both of which display light-activated ion channel activity, but not in BR, which only functions as a light-driven proton pump without detectable channel-like conductances [17]. Importantly, three out of the four charged TM2 residues are glutamates, i.e. negatively charged side-chains known to serve as binding sites for permeating cations in other channel proteins, such as voltage-gated Na<sup>+</sup> and Ca<sup>2+</sup> channels [24,25].

##### 4.1. Charge inversion substitutions

In agreement with an important role of the TM2 glutamates in ChR2 channel activity, replacement of residues E97, E90 and E101 by lysines, i.e. charge inversions at the respective positions, resulted in severe reductions of ChR2 conductance. Unlike the wild-type protein, these charge inversion mutants generated only tiny light-activated currents at pH 4.0, but not at pH 7.6 or 9.0 (Table 1). Together with the observed shift of  $V_{rev}$  into the far positive range, this is consistent with ChR2-YFP<sup>E97K</sup> and ChR2-YFP<sup>E101K</sup> mutants being partially conductive for H<sup>+</sup> but not Na<sup>+</sup>. Supporting this



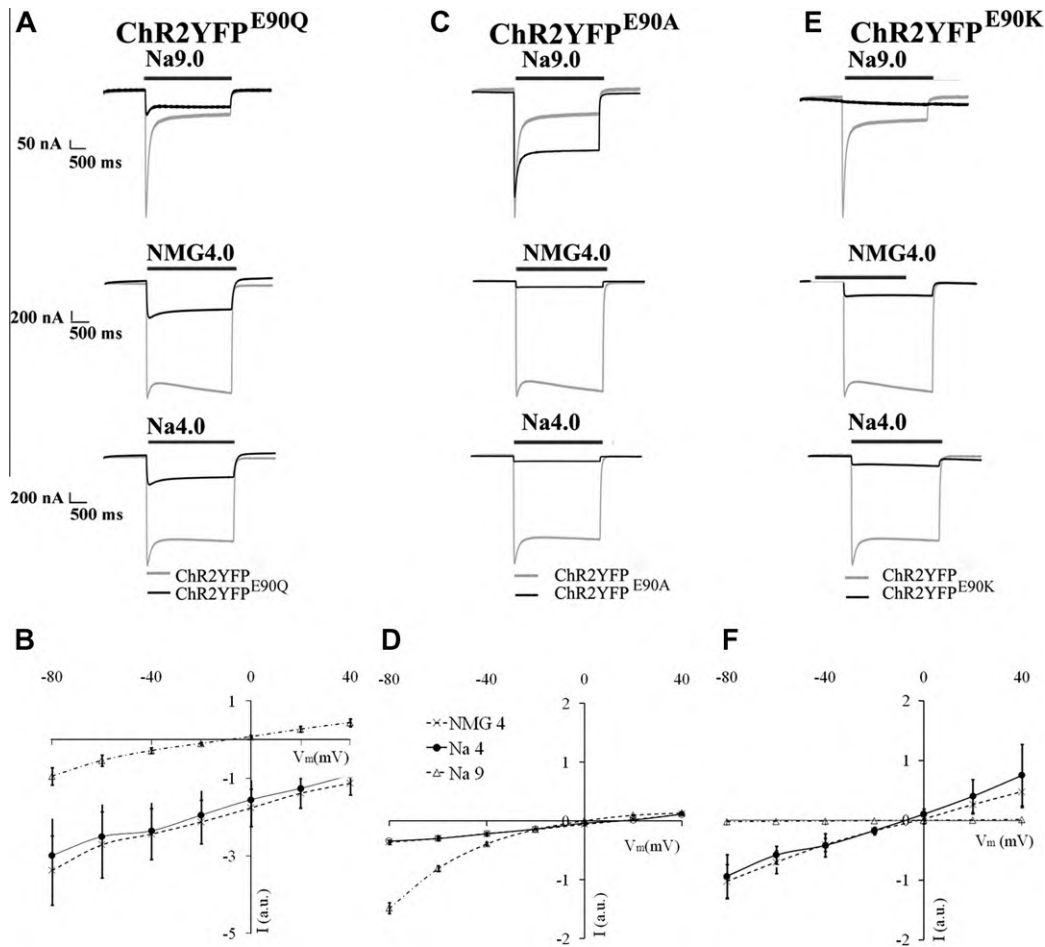


**Fig. 3.** Analysis of the  $\text{Na}^+$ - and  $\text{H}^+$ -currents carried by ChR2-YFP<sup>E90Q</sup>, ChR2-YFP<sup>E90A</sup> and ChR2-YFP<sup>E90K</sup>. (A, C and E) Current traces recorded from oocytes expressing ChR2-YFP<sup>E90Q</sup>, ChR2-YFP<sup>E90A</sup>, or ChR2-YFP<sup>E90K</sup> (black traces) or, for comparison, ChR2-YFP (gray traces) at  $V_m = -80$  mV in NMG4.0, Na9.0 and Na4.0 buffers. Note differently sized scale bars at Na9.0. Periods of illumination are indicated by black bars. (B, D and F) Normalized  $I/V$ -relationships of stationary photocurrents produced by ChR2-YFP<sup>E90Q</sup>, ChR2-YFP<sup>E90A</sup>, or ChR2-YFP<sup>E90K</sup>, respectively, in NMG4.0, Na9.0 and Na4.0. Current values were normalized to the current amplitudes recorded in Na4.0 at  $V_m = -60$  mV (a.u. = arbitrary units).

interpretation, comparison of the relative contributions of  $\text{Na}^+$  and  $\text{H}^+$  to the total current in Na4.0 and NMG4.0 superfused ChR2-YFP expressing oocytes revealed that at pH 4.0 >80% of the total current was carried by protons. In contrast, the currents recorded in Na7.6 were predominantly mediated by  $\text{Na}^+$  ions. Notably, the charge inversion mutant ChR2-YFP<sup>E90K</sup> also did not conduct any detectable currents in pH 9.0 or pH 7.6 buffers, suggesting that this mutant is similarly impaired in  $\text{Na}^+$  permeation. Together these findings provide evidence that glutamate residues within the predicted TM2 of ChR2 are important for the sodium conductance of ChR2.

#### 4.2. Polar substitutions

The importance of E97 and E101 is further supported by the observation that respective alanine substitutions resulted in strongly reduced ChR2 conductances [10], although the relative contributions of  $\text{Na}^+$  and  $\text{H}^+$  to the total current remained largely unchanged (cf. Fig. 2 and  $V_{\text{rev}}$  values in Table 1; and K.R. and V.E., unpublished data). This contrasts our findings with ChR2-YFP<sup>E90A</sup> which generated large currents in Na7.6 and Na9.0 buffers, suggesting that, unlike E97 and E101, E90 is not required for  $\text{Na}^+$  permeation. Conversely, at pH 4.0 ChR2-YFP<sup>E90A</sup> currents were significantly reduced compared to those of ChR2-YFP. Thus, the E90A substitution strongly reduces the  $\text{H}^+$  conductance. Consistent with this interpretation,  $V_{\text{rev}}$  of the light-induced currents recorded

at pH 4.0 was shifted to more negative values. The residual currents, however, appeared not to be carried by  $\text{Na}^+$ , since the  $I/V$  curves determined in buffers with or without  $\text{Na}^+$  were nearly identical. Interestingly, in Na4.0 and NMG4.0 buffers the  $I/V$  relations of ChR2-YFP<sup>E90A</sup> were almost indistinguishable from those of ChR2-YFP<sup>E90K</sup> (Fig. 3), suggesting that the negative charge of residue E90 is not needed for cation permeation. This conclusion is further supported by our analysis of ChR2-YFP<sup>E90Q</sup>, where replacement of the negatively charged side chain of E90 by a polar group of the same size did not qualitatively change the  $I/V$  curves under all buffer conditions analyzed, although average current amplitudes were reduced. This is consistent with spectroscopic data suggesting that E90 is protonated at least in the resting state of ChR2 [22].

#### 4.3. Ion selectivity

Notably, all charge inversion mutants analyzed retained some light-induced currents in acidic buffers. For ChR2-YFP<sup>E97K</sup> and ChR2-YFP<sup>E101K</sup>, currents were predominantly mediated by protons, as indicated by a positive  $V_{\text{rev}}$  comparable to ChR2-YFP. In contrast, the  $I/V$  relations of ChR2-YFP<sup>E90K</sup> were strikingly different. Although this mutant did not produce detectable light-induced currents at neutral or alkaline pH, at pH 4.0 its  $I/V$  curves were shifted leftwards with a  $V_{\text{rev}}$  close to 0 mV, consistent with changes in ion selectivity. Furthermore, our analysis of ChR2-YFP<sup>E90A</sup>

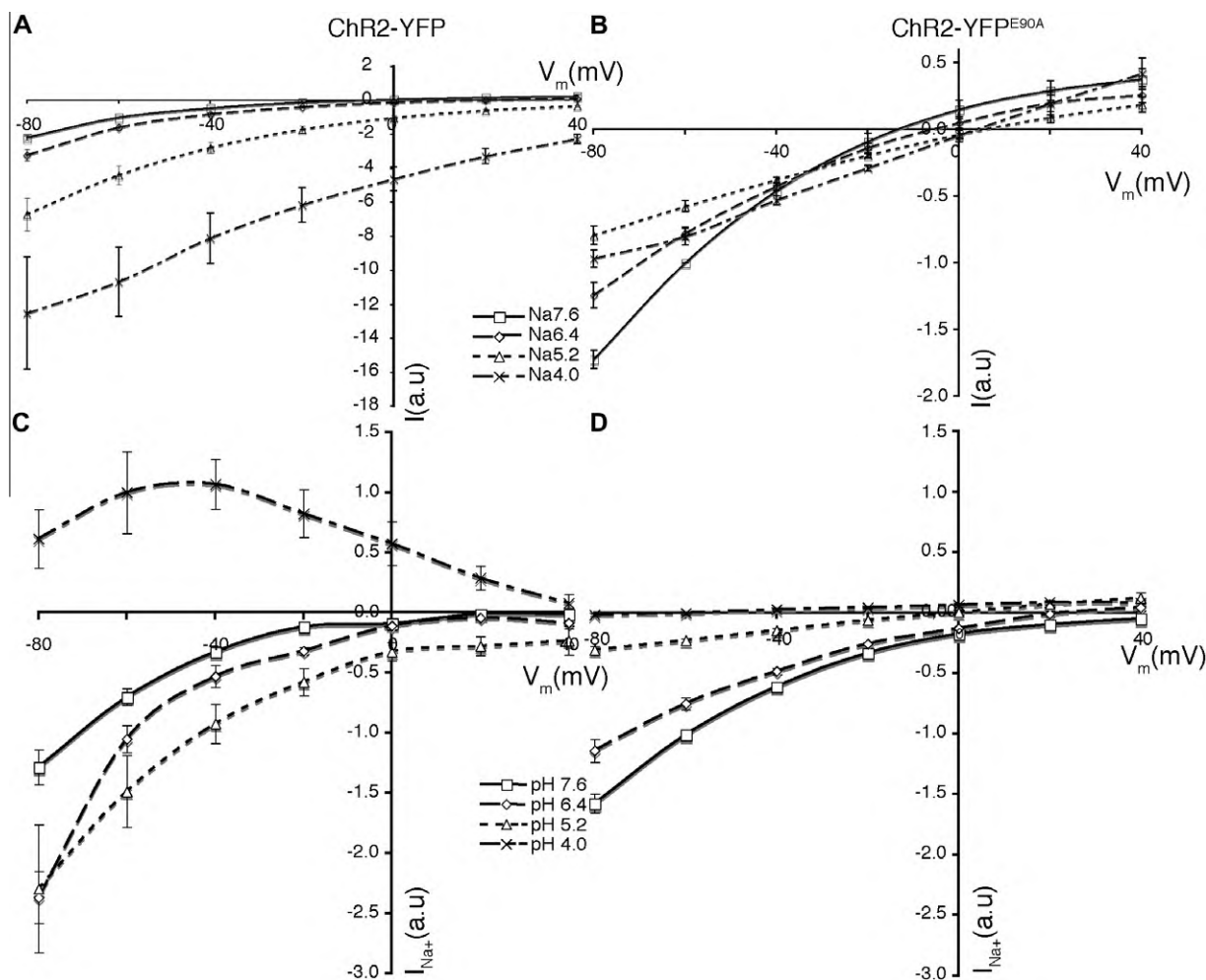


**Fig. 4.** pH-Dependence of  $H^+$ - and  $Na^+$ -mediated currents of ChR2-YFP and ChR2-YFPE90A. Normalized  $I/V$ -relationships of stationary photocurrents generated by (A) ChR2-YFP and (B) ChR2-YFPE90A in  $Na^+$ -buffer adjusted to pH values of 4.0, 5.2, 6.4 and 7.6. (C and D) Calculated  $Na^+$ -components of the light-induced currents as determined at the indicated pH from the difference in the stationary currents generated in the respective  $Na^+$  and NMG containing buffers (a.u. = arbitrary units).

suggests that this mutant is only poorly permeable for protons although its  $Na^+$  conductance appeared to be unchanged at neutral and alkaline pH. At low pH, however, ChR2-YFPE90A displayed only poor  $Na^+$  permeability, most likely due to protonation of residues different from E90.

In conclusion, our data provide evidence that negatively charged residues within TM2 are important for the light-induced channel activity of ChR2. In particular residue E90, positioned in the middle of the predicted TM2, appears to constitute a major determinant of cation selectivity. Clearly further experiments are required to fully understand how ChR2 functions as both proton pump and cation-selective channel.

## Appendix A. Supplementary data

Supplementary data associated with this article can be found, in the online version, at [doi:10.1016/j.bbrc.2011.06.024](https://doi.org/10.1016/j.bbrc.2011.06.024).

## References

- [1] G. Nagel, T. Szellas, W. Huhn, et al., Channelrhodopsin-2, a directly light-gated cation-selective membrane channel, *Proc. Natl. Acad. Sci. USA* 100 (2003) 13940–13945.
- [2] T. Suzuki, K. Yamasaki, S. Fujita, et al., Archaeal-type rhodopsins in *Chlamydomonas*: model structure and intracellular localization, *Biochem. Biophys. Res. Commun.* 301 (2003) 711–717.
- [3] C. Bamann, T. Kirsch, G. Nagel, et al., Spectral characteristics of the photocycle of channelrhodopsin-2 and its implication for channel function, *J. Mol. Biol.* 375 (2008) 686–694.
- [4] R. Henderson, P.N. Unwin, Three-dimensional model of purple membrane obtained by electron microscopy, *Nature* 257 (1975) 28–32.
- [5] W.A. Havelka, R. Henderson, J.A. Heymann, et al., Projection structure of halorhodopsin from *Halobacterium halobium* at 6 Å resolution obtained by electron cryo-microscopy, *J. Mol. Biol.* 234 (1993) 837–846.
- [6] J.K. Lanyi, B. Schobert, Structural changes in the L photointermediate of bacteriorhodopsin, *J. Mol. Biol.* 365 (2007) 1379–1392.
- [7] M. Kolbe, H. Besir, L.O. Essen, et al., Structure of the light-driven chloride pump halorhodopsin at 1.8 Å resolution, *Science* 288 (2000) 1390–1396.
- [8] G. Nagel, T. Szellas, S. Kateriya, et al., Channelrhodopsins: directly light-gated cation channels, *Biochem. Soc. Trans.* 33 (2005) 863–866.
- [9] K. Feldbauer, D. Zimmermann, V. Pintschovius, et al., Channelrhodopsin-2 is a leaky proton pump, *Proc. Natl. Acad. Sci. USA* 106 (2009) 12317–12322.
- [10] Y. Sugiyama, H. Wang, T. Hikima, et al., Photocurrent attenuation by a single polar-to-nonpolar point mutation of channelrhodopsin-2, *Photochem. Photobiol. Sci.* 8 (2009) 328–336.
- [11] T. Debon, P. Daenens, J. Tytgat, An improved fractionation and fast screening method for the identification of new and selective neurotoxins, *Neurosci. Res.* 24 (1996) 201–206.
- [12] M. Horiuchi, A. Nicke, J. Gomez, et al., Surface-localized glycine transporters 1 and 2 function as monomeric proteins in *Xenopus* oocytes, *Proc. Natl. Acad. Sci. USA* 98 (2001) 1448–1453.
- [13] F. Weinreich, P.G. Wood, J.R. Riordan, et al., Direct action of genistein on CFTR, *Pflügers Arch.* 434 (1997) 484–491.
- [14] B. Marquez-Klaka, J. Rettinger, Y. Bhargava, et al., Identification of an intersubunit cross-link between substituted cysteine residues located in the putative ATP binding site of the P2X1 receptor, *J. Neurosci.* 27 (2007) 1456–1466.
- [15] P. Berthold, S.P. Tsunoda, O.P. Ernst, et al., Channelrhodopsin-1 initiates phototaxis and photophobic responses in *Chlamydomonas* by immediate light-induced depolarization, *Plant Cell* 20 (2008) 1665–1677.

- [16] H. Wang, Y. Sugiyama, T. Hikima, et al., Molecular determinants differentiating photocurrent properties of two channelrhodopsins from *Chlamydomonas*, *J. Biol. Chem.* 284 (2009) 5685–5696.
- [17] R.H. Lozier, R.A. Bogomolni, W. Stoeckenius, Bacteriorhodopsin: a light-driven proton pump in *Halobacterium halobium*, *Biophys. J.* 15 (1975) 955–962.
- [18] B.R. Arenkiel, J. Peca, I.G. Davison, et al., In vivo light-induced activation of neural circuitry in transgenic mice expressing channelrhodopsin-2, *Neuron* 54 (2007) 205–218.
- [19] G. Nagel, M. Brauner, J.F. Liewald, et al., Light activation of channelrhodopsin-2 in excitable cells of *Caenorhabditis elegans* triggers rapid behavioral responses, *Curr. Biol.* 15 (2005) 2279–2284.
- [20] E.S. Boyden, F. Zhang, E. Bamberg, et al., Millisecond-timescale, genetically targeted optical control of neural activity, *Nat. Neurosci.* 8 (2005) 1263–1268.
- [21] S.P. Tsunoda, P. Hegemann, Glu 87 of channelrhodopsin-1 causes pH-dependent color tuning and fast photocurrent inactivation, *Photochem. Photobiol.* 85 (2009) 564–569.
- [22] E. Ritter, K. Stehfest, A. Berndt, et al., Monitoring light-induced structural changes of channelrhodopsin-2 by UV-visible and Fourier transform infrared spectroscopy, *J. Biol. Chem.* 283 (2008) 35033–35041.
- [23] A.M. Woodhull, Ionic blockage of sodium channels in nerve, *J. Gen. Physiol.* 61 (1973) 687–708.
- [24] S.H. Heinemann, H. Terlau, W. Stühmer, et al., Calcium channel characteristics conferred on the sodium channel by single mutations, *Nature* 356 (1992) 441–443.
- [25] T. Schlieff, R. Schonherr, K. Imoto, et al., Pore properties of rat brain II sodium channels mutated in the selectivity filter domain, *Eur. Biophys. J.* 25 (1996) 75–91.